PNAS RESEARCH ARTICLE | BIOPHYSICS AND COMPUTATIONAL BIOLOGY

Optimal strategies for correcting merotelic chromosome attachments in anaphase

Evgenii Kliuchnikov[a], Kenneth A. Marx[a], Valeri Barsegov[a,1], and Alex Mogilner[b,1]

Affiliations are included on p. 8.

Edited by Daniela Cimini, Virginia Polytechnic Institute and State University, Blacksburg, VA; received August 13, 2024; accepted December 27, 2024 by Editorial Board Member Rebecca Heald

Accurate chromosome segregation in mitosis depends on proper connections of sister chromatids, through microtubules, to the opposite poles of the early mitotic spindle. Transiently, many inaccurate connections are formed and rapidly corrected throughout the mitotic stages, but a small number of merotelic connections, in which a chromatid is connected to both spindle poles, remain lagging at the spindle's equator in anaphase. Most of the lagging chromatids are eventually moved to one or the other pole, likely by a combination of microtubules' turnover and the brute force of pulling by the microtubules' majority from the one pole against the microtubules' minority from the other pole. We use computer simulations from two stochastic models (1D and full 3D CellDynaMo model) combining force balances and microtubules' dynamics for the lagging chromatids to investigate what maximizes the percentage of segregated laggards. We find that a) brute force tug-of-war with slow (< 0.0001 s^{-1}) microtubules' detachment rate can move asymmetric laggards to the poles in limited time, b) rapid (> 0.01 s^{-1}) microtubules' detachment rate leads to a significant loss of the laggards, and c) intermediate (~ 0.001 s^{-1}) microtubules' detachment rate ensures higher than 90% accuracy of segregation. The simulations also shed light on the waiting time required to correct the merotelic errors in anaphase and on the roles of chromatid-attached microtubule number and Aurora B–mediated, spatially graded regulation of microtubule kinetics in anaphase.

anaphase | tug-of-war | merotelic errors | 3D computational modeling

Significance

Accurate chromosome segregation in mitosis depends on proper connections of sister chromatids to the opposite spindle poles. Transiently, many inaccurate connections are made and rapidly corrected throughout the mitotic stages, but a small number of dangerous merotelic connections, in which a chromatid is connected to both spindle poles, persist to anaphase. Most of these lagging chromatids are eventually resolved, but respective error correction mechanisms are unclear. We evaluate computationally the strategies optimizing the merotelic error correction and find that pure mechanical action is sufficient in moving asymmetric lagging chromatids to the poles but that mechanically sensitive microtubules' detachment with an optimal rate ~ 0.001/s is necessary to ensure higher than 90% error correction accuracy.

Segregation of chromosomes in mitosis is one of the most fundamental cell biological processes (1). Just before one of the last mitotic stages, anaphase, chromosomes—sister chromatids—are aligned at the spindle equator. At this point, each of the sister chromatids is connected, at the kinetochore (KT) located to the centromeric region of the chromatid, to a bundle of microtubules (MTs) called a K-fiber. One of the K-fibers stretches from the KT of one of the chromatids in this pair to one of the spindle poles, and another K-fiber from the sister KT to the opposite spindle pole. At the onset of anaphase, cohesion between the sister chromatids is dissolved, and shortening of the K-fibers due to disassembly of both MT ends at the KTs and poles drives the segregated sister chromatids poleward; this part of the process is called anaphase A. Concurrently, or at a slightly different time, anaphase B assists chromatid segregation by elongating the spindle, driving the poles apart and thereby increasing the distances between the chromatids and spindle equator. This process of anaphase, much more complex and nuanced than described here, has been studied for decades, yet underlying mechanisms are still under debate, especially for human cells (2–4).

Accurate chromatid segregation in anaphase—each of the sister chromatids must reach their respective opposite poles by the end of anaphase to equally divide the genome between two daughter cells—depends on accurate amphitelic KT–MT connections, in which MTs from one pole connect to one KT, while MTs from the other pole connect to the sister KT, established during early stages of mitosis (5). This accuracy is stunning: Only one out of thousands of chromatids in tens of dividing cells is missegregated (6). However, a 100% accurate connection is improbable to achieve. Two kinds of mistakes can be made: Syntelic error in which sister KTs connect to the same pole, and merotelic error (Fig. 1*A*), when one (or both) of the sister KTs connects to both poles. Both syntelic and merotelic errors are indeed made transiently in early stages of mitosis in great numbers, but most of them are corrected before anaphase by complex, yet, poorly understood mechanisms relying largely on MT turnover (6–9). The high eventual accuracy is important because chromosome missegregation could lead to cancer, miscarriages, death, and developmental defects (10).

Author contributions: E.K., K.A.M., V.B., and A.M. designed research; E.K. and A.M. performed research; E.K., K.A.M., V.B., and A.M. analyzed data; and E.K., K.A.M., V.B., and A.M. wrote the paper.

The authors declare no competing interest.

This article is a PNAS Direct Submission. D.C. is a guest editor invited by the Editorial Board.

[1]To whom correspondence may be addressed. Email: Valeri_Barsegov@uml.edu or mogilner@cims.nyu.edu.

This article contains supporting information online at https://www.pnas.org/lookup/suppl/doi:10.1073/pnas.2416459122/-/DCSupplemental.

Published January 30, 2025.

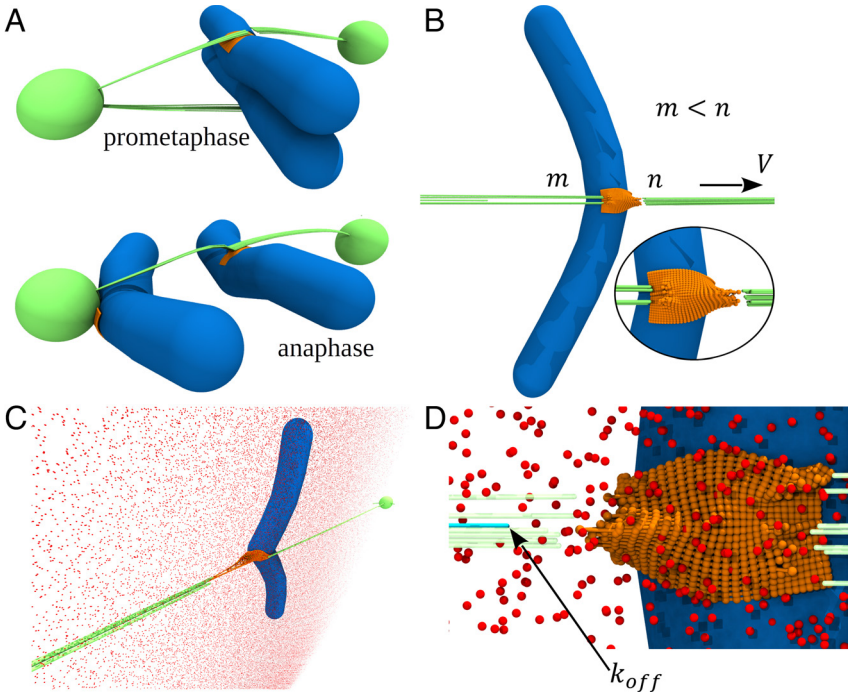

Fig. 1. Anaphase model: (*A*) Merotelic type of attachment during prometaphase (*Top*) and the resulting laggard chromatid (*Bottom*) illustrated by snapshots taken from CellDynaMo simulations. The spindle poles are represented as green spheres, the MTs as thin green cylinders, the chromatids as thick blue cylinders, and the KT as interconnected orange spheres. (*B*) An example of unbalanced merotelic attachments. Unequal numbers of MTs from each pole ($m < n$) result in the movement of the chromatid toward the majority of MTs. (*C*) Snapshot of a single chromatid during anaphase showing one of the poles with MTs, flexible KT, and molecules of Aurora B (red spheres) near the spindle equator. The Aurora B cloud is shown only in the narrow central cross-section region for better visualization. (*D*) A high-resolution view showing MT detachment (light blue) with the kinetic rate constant (off-rate) k_{off}.

Despite this early error correction, some merotelically attached chromatids at the spindle equator persist to anaphase (6, 11, 12): In healthy cells, up to 1% of chromatids at the onset of anaphase lag at the spindle equator. Crucially, less than 10% of these laggards missegregate (13); these cause aneuploidy and chromosomal instability in cancer cells (14), in which the numbers of both merotelic attachments at the anaphase onset and eventual laggards increase up to 100-fold (15). In this paper, we focus on a mechanism ensuring that more than 90% of merotelically attached chromatids at the anaphase onset are moved to one of the spindle poles by the end of anaphase (16, 17).

Such a mechanism is hypothesized to be a combination of the brute force tug-of-war and MT turnover mechanisms (12, 18–20). The former relies on the force balance: If unequal numbers of MTs from the opposite poles are connected to the single KT (Fig. 1*B*) on the lagging chromatid, then the greater number of MTs from the first pole overcomes the pull from the smaller number of MTs from the second pole, and the resulting shortening of the majority of MTs from the thicker K-fiber drives the chromatid to the first pole. The latter mechanism is that KT–MT detachments assist the tug-of-war if these detachments amplify the inequality of two opposing K-fibers by increasing the difference between the numbers of opposing MTs. Logical questions that these hypotheses raise are as follows: How effective could a pure tug-of-war mechanism be in the absence of the KT–MT detachments? Do faster KT–MT detachments jeopardize the chromatid segregation or accelerate it? Can force sensitivity of the KT–MT links be beneficial for resolving merotelic connections?

One additional important aspect of this problem concerns the role of Aurora B kinase in the rescue of the laggards in anaphase (16). Recent experiments demonstrate that Aurora B rapidly relocates to the spindle equator (20) at the onset of anaphase, and prevention of this relocation results in a significant increase in the number of laggards (17). The authors of Ref. 17 suggested that Aurora B activity at the equator promotes the phosphorylation of KT substrates, destabilizing MTs on the "incorrect" side more efficiently. It is not clear whether this works for "symmetric" merotelic attachments with equal MT numbers from the opposite poles—would not there be a high chance of complete MT detachment from both sides? Alternatively, the authors of Ref. 16 observed that Aurora B on the spindle equator stabilizes MT attachments, securing the misbalance of the MT numbers from the opposite poles in asymmetric merotelic attachments and allowing the pure tug-of-war to work. However, would not the symmetric merotelic attachments remain stuck on the equator in this case?

Here, we use computational modeling to answer these questions, and we find that both mechanics and kinetics of KT–MT connections maximize the rate of rescuing the lagging chromatids in anaphase. Computer simulations and intuition from theoretical models have been instrumental in understanding mitosis in general and behavior of the chromatids at the spindle equator in particular (21–24). Following the pioneering ideas introduced in (18), we use modeling to find that when the KT–MT detachment frequency is too high, no chromatid reaches a pole; when this frequency is too low, the chromatid does (does not) reach the pole for the asymmetric (symmetric) merotelic connections; and at an intermediate detachment frequency, both types of merotelic connections are successfully resolved. We further find that a) if KT–MT connections are slip bonds, the rate of success dramatically improves, b) increasing the detachment rate at the spindle equator optimizes segregation of the initially symmetric merotelic chromatids, and c) pure tug-of-war without MT turnover is effective for initially asymmetric merotelic chromatids.

Materials and Methods

We consider a chromatid lagging at the spindle equator in the beginning of anaphase (25) (Fig. 1*C*), with a K-fiber formed by n MTs connecting the single KT to the right pole and a K-fiber of m MTs connecting this KT to the left pole

(Fig. 1*B*). Following reported data (26, 27), in the model, new KT–MT connections are not allowed in anaphase. We first simulate a simplified 1D model, which is inspired by (18), and which allows rapid and thorough screening of key parameters. To find the force balance and resulting chromatid movement, we follow well-established models based on the notion of the force(f)-velocity(V) relation for the MT plus-ends (18, 21–24). Namely, the pulling force applied to the MT plus-end, $f = F_0\left(1 - V/V_0\right)$, depends on F_0 –the force that stalls the MT plus-end shortening, V_0 –the force-free plus-end shortening rate, and V –the actual plus-end shortening rate, which slows down by the applied pulling force f (Fig. 1*B*). This force–velocity relation can be rewritten as $V = V_0\left(1 - f/F_0\right)$. If the pulling force f is greater than F_0, V is negative meaning that the MT elongates if the force on its plus-end is large enough. In support of this notion, when a merotelic chromatid glides to one of the poles, a small number of elongating connected MTs survive on the incorrect side (28), suggesting that at least some MTs do not detach but rather polymerize under an overwhelming force from the other side. In this model, each KT-connected MT detaches with the force-dependent off-rate modeled, according to experimental data, as $k_{off} = k_{off,0}exp\left(\alpha f/F_0\right)$, where $k_{off,0}$ is the base (force-free) detachment rate, and α is the force sensitivity parameter (29–31). In this simplified model, we do not specify whether the force–velocity relation describes only the MT plus-end behavior, or that it is combined with motors and linkers on the KT (4). Similarly, for simplicity, we neglect shortening of the K-fiber through MT depolymerization at their minus-ends (4). Finally, the measured force–velocity relations are characterized by various nonlinearities, but it was shown that when several force generators act in parallel, the linear approximation that we use and that greatly simplifies the simulations is accurate (30).

The force balance on the chromatid, if one neglects viscous resistances, is given by equating the total pulling forces from the left and right: $mf_- = nf_+ = F$, where f_- and f_+ are the forces per MT at the left and right of the KT, respectively, and F is the intra-KT tension. The evidence of such tension is the observed stretching of the merotelically attached KT due to pulling forces toward opposite poles (32). Further, more subtle evidence for the force balance equation comes from the observation that the leading KT part is stretched less than its trailing part (33). Indeed, if $m < n$, then $f_- > f_+$. Substituting the force–velocity relation into the force balance equation, we obtain the resulting chromatid velocity (Fig. 1*B*) driven by the tug-of-war between the majority of n MTs from one pole against m MTs from the opposite pole: $V = V_0\frac{n-m}{n+m}$. Furthermore, substituting the force balance equation into the formula for the detachment rate, we find the resulting *net* frequencies of MT detachments from the n-MTs K-fiber, $k_{n,m\to n-1,m} = nk_{off,0}exp\left(\frac{2\alpha m}{n+m}\right)$, and from the m-MTs K-fiber, $k_{n,m\to n,m-1} = mk_{off,0}exp\left(\frac{2\alpha n}{n+m}\right)$. In these 1D model–based simulations, the chromatid velocity can be found at each time step given numbers n and m; these numbers are then updated stochastically (using the Gillespie algorithm) based on the detachment frequencies (more detail in *SI Appendix*).

The rationale for using the 1D model is that this simplified model helps to build intuition and illuminate a physical picture of a complex process. Once we build our intuition, we then support this intuition with full 3D simulations (Fig. 1 *C* and *D*), using CellDynaMo, where initially two K-fibers from the opposite poles connect to the deformable elastic KT on the chromatid. Like in the 1D model, in the CellDynaMo simulations, the KT–MT connections break with the force-dependent rates, and MT growth and shortening are governed by the linear force–velocity relation. However, in the 3D model, the explicit 3D geometry of the chromatid and KT and MTs as well as elastic and viscous forces, which are absent in the 1D model, are also considered. The chromatid has large deformable arms that produce viscous resistance to their movement, which is added to the MT-generated force balance. In this study, only a single laggard chromatid is simulated. The spindle poles are kept immobile in the simulations, and so the cell shape does not affect the results. The MT plus-ends in the simulations are connected to the KT by elastic Ndc-80 linkers, which disconnect with force-dependent frequencies based on the degree of phosphorylation regulated by the Aurora B enzyme molecules concentrated around the spindle equator. Details of the simulations are described in *SI Appendix* and in Refs. 34, 35. In both 1D and 3D models'-based simulations; we use parameters gleaned from the published experimental data (*SI Appendix*, Tables S1 and S2).

Results

The Slip Character of the KT–MT Bond Optimizes the Merotelic Resolution. From here on we will use the term "resolved" for the chromatid moved from the equator to either the left or right pole. We will use the term "success" for the chromatid resolved within a given time interval, and the term "optimal" for the parameter set maximizing the successes' percentages. (Note that this limited definition of success does not discriminate between the chromatid moving to the same/opposite pole to which the sister chromatid moved. In *SI Appendix*, Fig. S4*C* we show more nuanced simulation results. First, we start building intuition about the optimal strategy using the simplified 1D model without the effect of Aurora B.

In Fig. 2 *A*–*C*, we report the results of 1D model–based simulations obtained by varying initial ratios of the left MT number-to-right MT number (10:1, 10:3, 10:5, 10:7, and 10:10) and varying base MT detachment frequencies (force-free detachment rates). We consider 3 cases for the KT–MT connections: The catch-bond ($\alpha < 0$, connection becomes stronger with the increased force on the bond), the force-independent regular bond ($\alpha = 0$), and the slip bond ($\alpha > 0$, connection becomes weaker with the increased force on the bond). These noncovalent bond scenarios are depicted in Fig. 2 *A*–*C*, respectively. In these simulations, the limiting time for the successful resolution was set to be equal to ~4 min—the characteristic duration of anaphase (36). This is not a very strict constraint because for the chosen model parameters, the time needed to shorten a K-fiber without any opposition from the opposing MTs is only ~2 min. The tug-of-war of 10 against 1 or 3 MTs under this condition is fast enough to resolve the merotelic attachment without any MT detachments, as is evident from Fig. 2 *A*–*C*, but not more symmetric attachments.

Looking at initially less asymmetric merotelic attachments for the catch bond (Fig. 2*A*), all other cases end in failure. The reason is that the total force on the KT to the right is equal to the total force to the left, so for the majority of MTs from the one side the force per MT is smaller than that for the minority of MTs from the other side. The catch bond then makes the minority of MTs attach stronger. The net effect is equalizing the MT numbers from both sides, which keeps the lagging chromatid stuck near the equator.

For the force-independent regular bond (Fig. 2*B*), there is a small chance of success for more symmetric merotelic attachments. This chance of success dramatically increases for the slip bond (Fig. 2*C*). The reason is that in this regime, the MT number asymmetry tends to increase because for the majority of MTs from one side, the force per MT is equal to the total force divided by the greater MT number, and so this force is smaller than the force per MT for the minority of MTs from the other side, which is equal to the same total force divided by the smaller MT number. The slip bond then makes the minority of MTs attach weaker. The net effect is enhancing the MT number differences from both sides, which accelerates the lagging chromatid movement to one of the poles. This effect is similar to the force-dependent tug-of war of molecular motors pulling in opposite directions, which tends to break the balance in favor of a unidirectional motion (37). The force sensitivity parameter α in the simulations was chosen to be on the order of this parameter measured experimentally (31); we also varied this parameter (*SI Appendix*, Fig. S1) to demonstrate that increasing force sensitivity improves the error correction, but not dramatically. In the remainder of this paper, we consider only slip bonds, which demonstrate much better results than the other two bond cases.

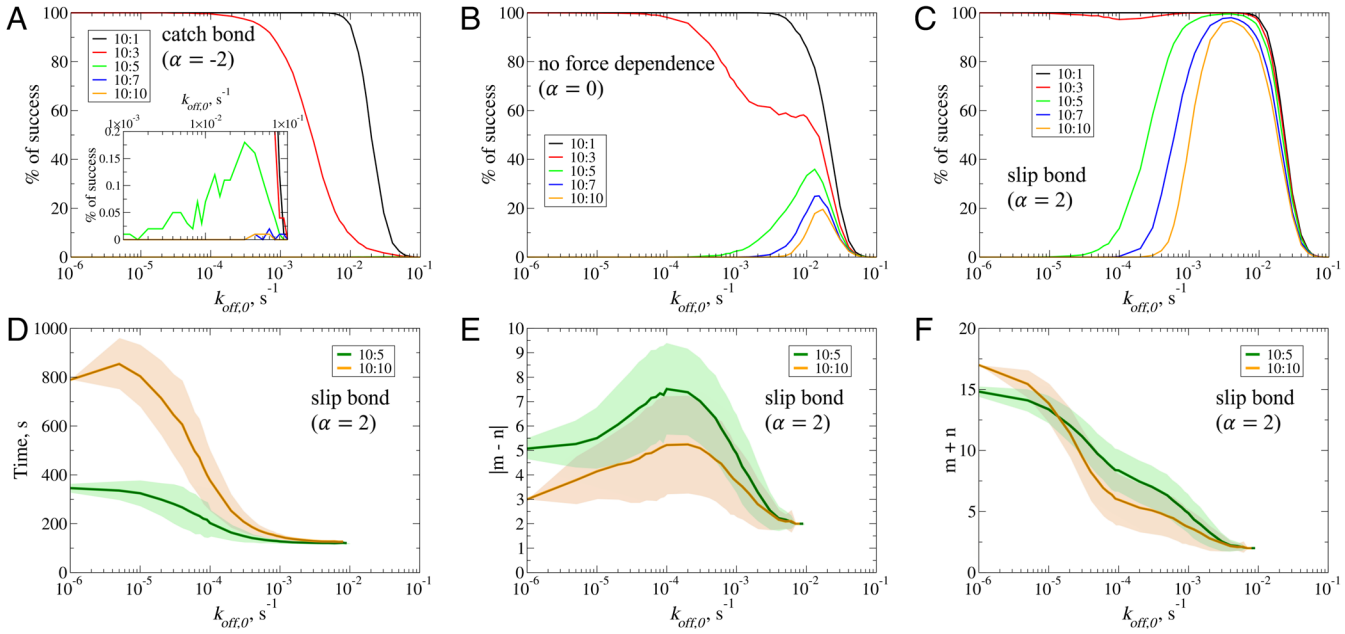

Fig. 2. Dependence of the chromatid dynamics on mechanical properties of the KT–MT bond in the 1D model: (*A–C*) Percentage of chromatids reaching one of the poles in the case of the catch bond (*A*: $\alpha = -2$), regular bond with no force dependence (*B*: $\alpha = 0$) and the slip bond (*C*: $\alpha = 2$) as a function of $k_{off,0}$. The simulation for the cases of ratios of MT numbers m: $n = 10$: 1 (black), 10:3 (red), 10:5 (green), 10:7 (blue), and 10:10 (orange) are shown. (*D*) Time required for the chromatid to reach one of the poles (first arrival time). (*E*) Difference between MTs from the opposite sides $|m-n|$ at the first arrival time (time moment when a chromatid reaches one of the poles). (*F*) Total numbers of MTs left from both poles $m + n$ at the first arrival time. In panels *D–F*, the averages and SD from the simulations are shown as functions of $k_{off,0}$ only for the case of the slip bond and for the cases of ratios of MTs m: $n = 10$: 5 (green) and 10:10 (orange). For each panel, the results from a total of 10,000 calculations statistics are shown. The equator-to-pole distance is 10 μm.

If the Time to Resolve the Lagging Merotelic Chromatid Is Limited, Then There Is an Optimal KT–MT Detachment Frequency. For all force dependencies (Fig. 2 *A–C*) and significant merotelic asymmetry (case 10:1), for small $k_{off,0}$ the chromatid has time to reach the pole as a result of the pure tug-of-war; the majority of MTs shorten rapidly enough against a small number of MTs from the opposite pole, so no MT detachment is necessary. Very high $k_{off,0} \sim 0.1\ s^{-1}$ makes the success percentage plunge because at such detachment rates, there is the danger that all MTs detach from even the majority side before the chromatid reaches the pole. This upper limit of $k_{off,0}$ is similar for more initially asymmetric attachments. For these initially asymmetric attachments, the detachment rates below $k_{off,0} \sim 0.001\ s^{-1}$ (Fig. 2 *B* and *C*) lead to the failure to resolve the chromatid because there are not enough MTs detaching from the minority side, which keeps the resulting chromatid velocity too low to reach a pole in the limited time.

These conclusions are underlined by the statistics shown in Fig. 2 *D–F*, where we increased the limiting time up to ~ 15 min, to account for the observed longer time in anaphase with merotelic laggards (12, 38). Fig. 2*F* demonstrates that the total MT number from both sides ($m + n$) decreases with $k_{off,0}$ making high detachment frequencies risky. On the other hand, low detachment frequencies lead to greater times needed to resolve the lagging chromatid (Fig. 2*D*), especially for more initially symmetric attachments, as significant asymmetry needed to pick up speed is not developed for longer time. Therefore, these results suggest that the cell in anaphase must compromise between fast and unsafe and slow and safe regimes.

Fig. 2*E* illustrates the reason for the optimal intermediate detachment rate: The average difference between MT numbers from the opposite poles ($|m-n|$) reaches maximum at an intermediate $k_{off,0}$. A rough estimate of this optimal intermediate detachment rate can be obtained as follows. For the majority of MTs on one side, not "feeling" much the force effect, it takes time $t_1 \sim ln(n)/k_{off,0}$ (on average) to disassemble. For the minority of MTs on the other side feeling the force effect, it will take time $t_2 \sim ln(m)e^{-2\alpha}/k_{off,0}$ (on average) to disassemble. The optimal time should be longer than t_2 but shorter than t_1. While the MTs detach, the chromatid moves with the speed $V \sim V_0(n-m)/(n+m) \sim cV_0$, where $c < 1$. The time required to move distance L (half-spindle length) is $t \sim L/(cV_0)$, and $t_2 < t < t_1$. Thus, we obtain $[cln(m)V_0/L]e^{-2\alpha} < k_{off,0} < [cln(n)V_0/L]$. As the logarithm of the characteristic MT number is on the order of 2-3-4, and $c < 1$, this inequality approximately simplifies to $(V_0/L)e^{-2\alpha} < k_{off,0} < (V_0/L)$. Thus, the order of magnitude of the optimal $k_{off,0}$ is simply the inverse time needed to move the chromatic across half the spindle force-free, and the width of the range of frequencies allowing successful symmetric merotelic resolution is about an order of magnitude, as the factor $e^{-2\alpha} \sim 0.1$.

In *SI Appendix*, Fig. S2, we show how the results depend on the waiting time limit and on spindle size. If the waiting time decreases, the upper limit of $k_{off,0}$ allowing successful resolution is almost unchanged (*SI Appendix*, Fig. S2 *A–C*), in agreement with the rough estimate obtained above. However, the lower limit of $k_{off,0}$ allowing successful resolution increases because shorter waiting time would not allow the tug-of war to resolve in time. Thus, the shorter the waiting time, the more fine-tuned the optimal detachment frequency must be, and even asymmetric merotelic attachments cannot be resolved by the pure tug-of-war. The smaller the spindle size, the wider the range of the allowed frequencies, with the upper limit shifted to the right (*SI Appendix*, Fig. S2 *D* and *E*), in agreement with the above rough estimate.

For Asymmetric Merotelic Attachments, It Does Not Matter Whether the Detachment Frequency Is Lower or Higher at the Spindle Equator, While the Fate of Symmetric Merotelic Attachments Is Modestly Improved If the Detachment Frequency Is Higher at the Spindle Equator. In Fig. 3, we examine the effect of Aurora B in the simplified 1D model by asking what changes the

process if $k_{off,0}$ is either lowered or elevated near the spindle equator, or near the poles? Hence, we consider 4 cases: Case 1, $k_{off,0}$ is lowered at the equator; Case 2, $k_{off,0}$ is lowered near the poles; Case 3,$k_{off,0}$ is elevated at the equator; and Case 4, $k_{off,0}$ is elevated near the poles (Fig. 3). Three conclusions can be reached by inspecting Fig. 3. First, lowering or elevating the detachment frequency locally simply shifts the success curve right or left, respectively. So, for example, if $k_{off,0}$ at the anaphase onset is too high, risking all MTs detaching too soon, then Aurora B should be used to lower the detachment frequency locally. Second, for the initially asymmetric connection, it does not matter at which location the detachment frequency is lowered or elevated. Third, for the initially symmetric connection, the range of optimal $k_{off,0}$ becomes wider (on the slower detachment frequency side) if the detachment frequency k_{off} is higher near the equator and the corresponding time to reach the pole (arrival time) is becoming shorter. The explanation for this last result is that it is more optimal to detach a minority of MTs sooner, creating the MT number asymmetry and allowing the tug-of-war to drive the chromatid to the pole faster, while lowering the detachment frequency near the pole, thereby preventing the danger of complete MT detachment. Finally, the time to resolve the chromatid is not very sensitive to the spatial patterning of the detachment frequency.

The Results Are Not Sensitive to the Total Number of the Initially Attached MTs; However, If the Initial MT Number Is Very Small, These KT–MT Connections Must Be Stabilized. Finally, we use the 1D model–based simulations to investigate the dependence of the successful resolution on the total MT number ($m + n$), comparing cases with the same initial MT asymmetry but with different total MT number (10:5 vs. 6:3 vs. 2:1) and (10:10 vs. 6:6 vs. 2:2); see Fig. 4. The intuitive result is that higher number $m + n$ is better in terms of the higher upper limit of the allowable values of $k_{off,0}$ for success because too few MTs increase the chance of all MTs accidentally detaching at higher detachment frequencies. Comparison of Fig. 4 and *SI Appendix*, Fig. S3, shows that the obtained results are not very sensitive to the choice of the width of the region at the spindle equator where the detachment frequency is lowered or elevated.

3D Simulations with Aurora B Stochastic Phosphorylating Action, Deformable KTs, and Viscous Resistance to Chromatid Arms Confirm the Conclusions of the 1D Model. Finally, we turn to full 3D simulations using CellDynaMo, with explicit modeling of the Aurora B stochastic action of phosphorylating KT–MT linkers and respective grading of the MT detachment rate, deformable elastic KTs, and large, viscous resistance-inducing, chromatid arms. Figs. 5 and 6 (initially symmetric and asymmetric merotelic attachments, respectively) demonstrate the following. a) When the overall base detachment frequency is too high, the chromatid does not reach a pole for any initial MT numbers m and n (Figs. 5 *D* and 6 *D*) because all MTs detach before the chromatid reaches a pole. b) When the overall detachment frequency is too low, the chromatid reaches the pole due to the tug-of-war for the asymmetric merotelic connection (Fig. 6*D*), but does not have enough time to reach a pole for the symmetric merotelic connection (Fig. 5*D*). c) When the overall detachment frequency is optimal, which is the intermediate case, both types of merotelic connections are successfully resolved. Note also that the CellDynaMo-based simulations vividly illustrate the important effect of the slip bond: The asymmetry of the MT numbers m and n from the opposite poles is amplified over time.

Discussion

Our simulations lead to the following conclusions: 1) The slip bonds between KTs and MTs significantly increase the chance for moving lagging anaphase chromatids toward one of the poles at moderate KT–MT detachment frequency, by increasing the

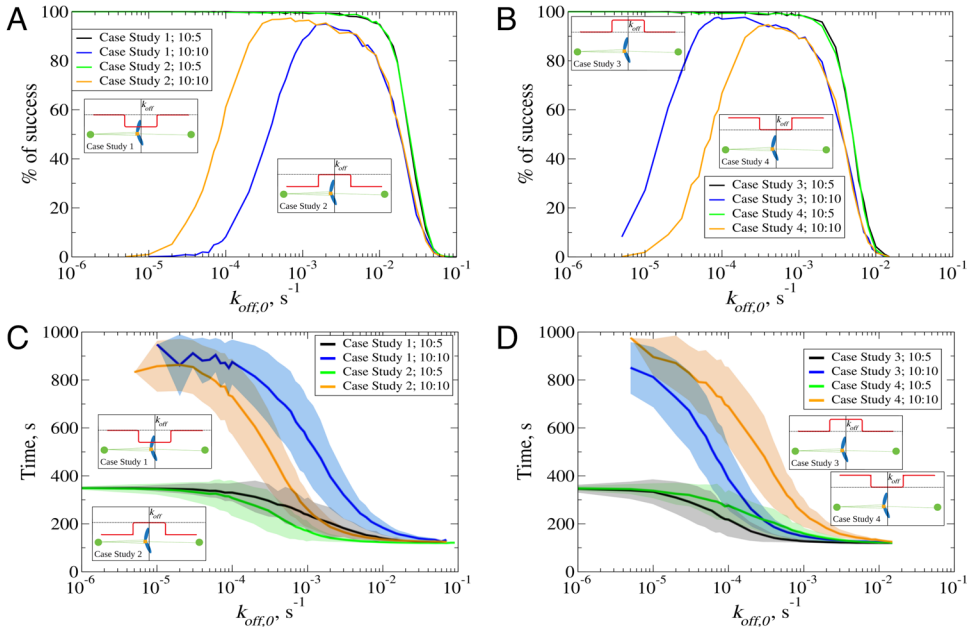

Fig. 3. Impact of microtubule numbers from opposite poles on chromatid dynamics during anaphase in the presence of Aurora B from the 1D model: (*A*) Percentage of success for Case Study 1 and MT ratio m: $n = 10$: 5 (black), Case Study 1 and MT ratio m: $n = 10$: 10 (blue), Case Study 2 and MT ratio m: $n = 10$: 5 (green), and Case Study 2 and MT ratio m: $n = 10$: 10 (orange). (*B*) Percentage of success for Case Study 3 and MT ratio m: $n = 10$: 5 (black), Case Study 3 and MT ratio m: $n = 10$: 10 (blue), Case Study 4 and MT ratio m: $n = 10$: 5 (green), and Case Study 4 and MT ratio m: $n = 10$: 10 (orange). (*C*) Time required for the chromatid to reach one of the poles (first arrival time) for Case Study 1 and MT ratio m: $n = 10$: 5 (black), Case Study 1 and MT ratio m: $n = 10$: 10 (blue), Case Study 2 and MT ratio m: $n = 10$: 5 (green), and Case Study 2 and MT ratio m: $n = 10$: 10 (orange). (*D*) The first arrival time (time required for the chromatid to reach one of the poles) for Case Study 3 and MT ratio m: $n = 10$: 5 (black), Case Study 3 and MT ratio m: $n = 10$: 10 (blue), Case Study 4 and MT ratio m: $n = 10$: 5 (green), and Case Study 4 and MT ratio m: $n = 10$: 10 (orange). For each panel, the results from 10,000 calculations statistics are shown as functions of $k_{off,0}$ only for the slip bond. The equator-to-pole distance is 10 μm. The spatial profiles for the KT–MT detachment rates across the spindle for four case studies are illustrated in the *Insets*.

asymmetry of the MT numbers in opposite K-fibers; 2) When the KT–MT detachment frequency is too high (> 0.01 s^{-1}), the chromatid does not reach a pole for any initial MT numbers because all connections to K-fibers are lost too soon. When the KT–MT detachment frequency is too low (< 0.0001 s^{-1}), the chromatid does (does not) reach the pole due to the pure tug-of-war for the asymmetric (symmetric) merotelic connections. When the KT–MT detachment frequency is optimal, which is the intermediate detachment frequency case (~0.001 s^{-1}), both types of merotelic connections can be resolved with higher than 90% success rate; 3) Spatial grading of the KT–MT detachment frequency does not matter for asymmetric merotelic connections, but for symmetric merotelic connections, the range of KT–MT detachment frequencies for successful resolution increases if the KT–MT detachment frequency is elevated at the spindle equator; 4) The waiting time for the lagging chromatid resolution increases with the decreasing KT–MT detachment frequency from a few minutes at high frequency (~0.01 s^{-1}) to 10 to 15 min for less asymmetric merotelic connections at low frequency (~0.0001 s^{-1}); and 5) Small (< 5) initial values of the total numbers of MTs merotelic connections worsens the outcome at finite KT–MT detachment frequency because of the danger of losing all KT–MT connections. This last prediction is supported by the observation (39) that complete KT–MT occupancy favors the segregation of merotelic attachments.

The evidence that the MT numbers attached to a merotelic KT could decrease in anaphase is indirect (17, 38): Initially, a stretched KT on the spindle equator relaxes when pulled to one of the poles. A straightforward interpretation of these results is that MTs from the "wrong" pole detach, relieving the intra-KT tension. (Note that the model makes a valuable quantitative prediction: The intra-KT stretch, which is simpler to measure than the MT numbers in K-fibers, should anticorrelate with the MT number imbalance).

Purely Mechanical Tug-of-War Can Effectively Resolve Merotelic Attachments Without KT–MT Detachments If Incomplete Error Correction Happens Before Anaphase. If there are no KT–MT detachments in anaphase, how viable is the purely mechanical tug-of-war as the error-correction mechanism? Less than 10% of the laggards at the anaphase onset missegregate (13), so the cell uses a strategy ensuring higher than 90% success rate. The optimal strategy for resolving the merotelic connections in anaphase depends on two parameters: a) the fraction of symmetric versus asymmetric connections and b) the waiting time the cell can afford. In human cells, the characteristic number of MTs per KT is ~15 (40). Assuming the Poisson distribution of this number with 15 MTs per KT on average, ~7% of the merotelic connections would be completely symmetric at the onset of anaphase (*SI Appendix*). However, according to our model, not only perfectly symmetric laggards but also 10 to 7 and even 10 to 5 laggards (MT numbers from two poles) will not be resolved within 15 min time. However, if the affordable waiting time is shorter, then even slightly asymmetric merotelic connections will not be resolved. Estimates in *SI Appendix* show that if the waiting time is ~5 min, then only ~65% of the merotelic attachments will be resolved.

If the earlier error correction mechanisms work toward increasing the MT numbers' asymmetry, and the chromatids lagging at anaphase have different average numbers of MTs connected to sister KTs, then the success rate of the pure tug-of-war mechanism

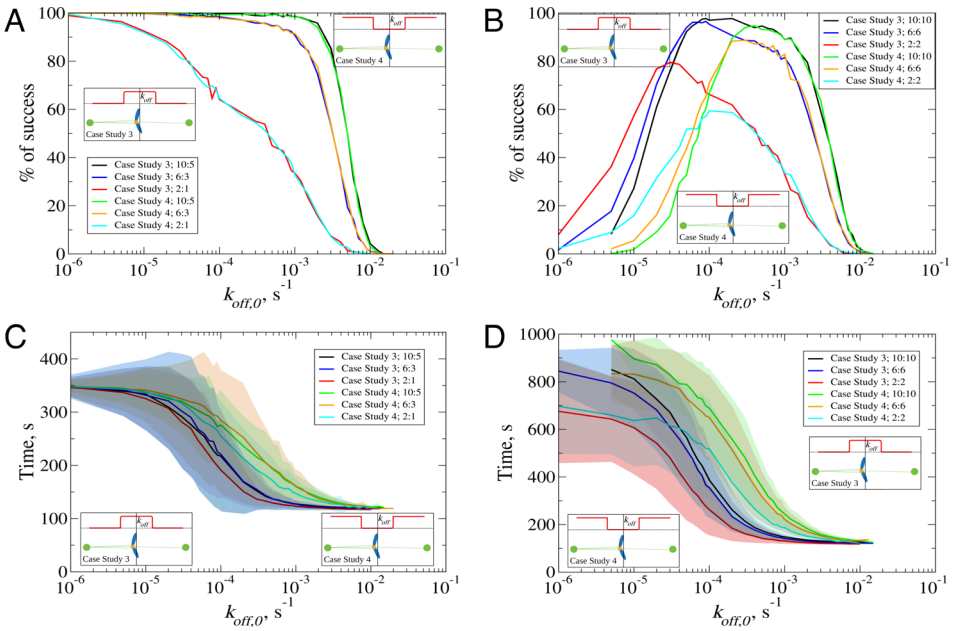

Fig. 4. Impact of microtubule numbers from opposite poles on chromatid dynamics from the 1D model: (*A*) Percentage of success for Case Study 3 and MT ratio m: n = 10: 5 (black), Case Study 3 and MT ratio m: n = 6: 3 (blue), Case Study 3 and MT ratio m: n = 2: 1 (red), Case Study 4 and MT ratio m: n = 10: 5 (green), Case Study 4 and MT ratio m: n = 6: 3 (orange), and Case Study 4 and MT ratio m: n = 2: 1 (light blue). (*B*) Percentage of success for Case Study 3 and MT ratio m: n = 10: 10 (black), Case Study 3 and MT ratio m: n = 6: 6 (blue), Case Study 3 and MT ratio m: n = 2: 2 (red), Case Study 4 and MT ratio m: n = 10: 10 (green), Case Study 4 and MT ratio m: n = 6: 6 (orange), and Case Study 4 and MT ratio m: n = 2: 2 (light blue). (*C*) Time required for the chromatid to reach one of the poles (first arrival time) for Case Study 3 and MT ratio m: n = 10: 5 (black), Case Study 3 and MT ratio m: n = 6: 3 (blue), Case Study 3 and MT ratio m: n = 2: 1 (red), Case Study 4 and MT ratio m: n = 10: 5 (green), Case Study 4 and MT ratio m: n = 6: 3 (orange), and Case Study 4 and MT ratio m: n = 2: 1 (light blue). Panel (*D*) The first arrival time (time required for the chromatid to reach one of the poles) for Case Study 3 and MT ratio m: n = 10: 10 (black), Case Study 3 and MT ratio m: n = 6: 6 (blue), Case Study 3 and MT ratio m: n = 2: 2 (red), Case Study 4 and MT ratio m: n = 10: 10 (green), Case Study 4 and MT ratio m: n = 6: 6 (orange), and Case Study 4 and MT ratio m: n = 2: 2 (light blue). For each panel, the results from 10,000 calculations statistics are shown as functions of $k_{off,0}$ only for the slip bond. The equator-to-pole distance is 10 μm. The spatial profiles for the KT–MT detachment rates across the spindle for four case studies are illustrated in the *Insets*.

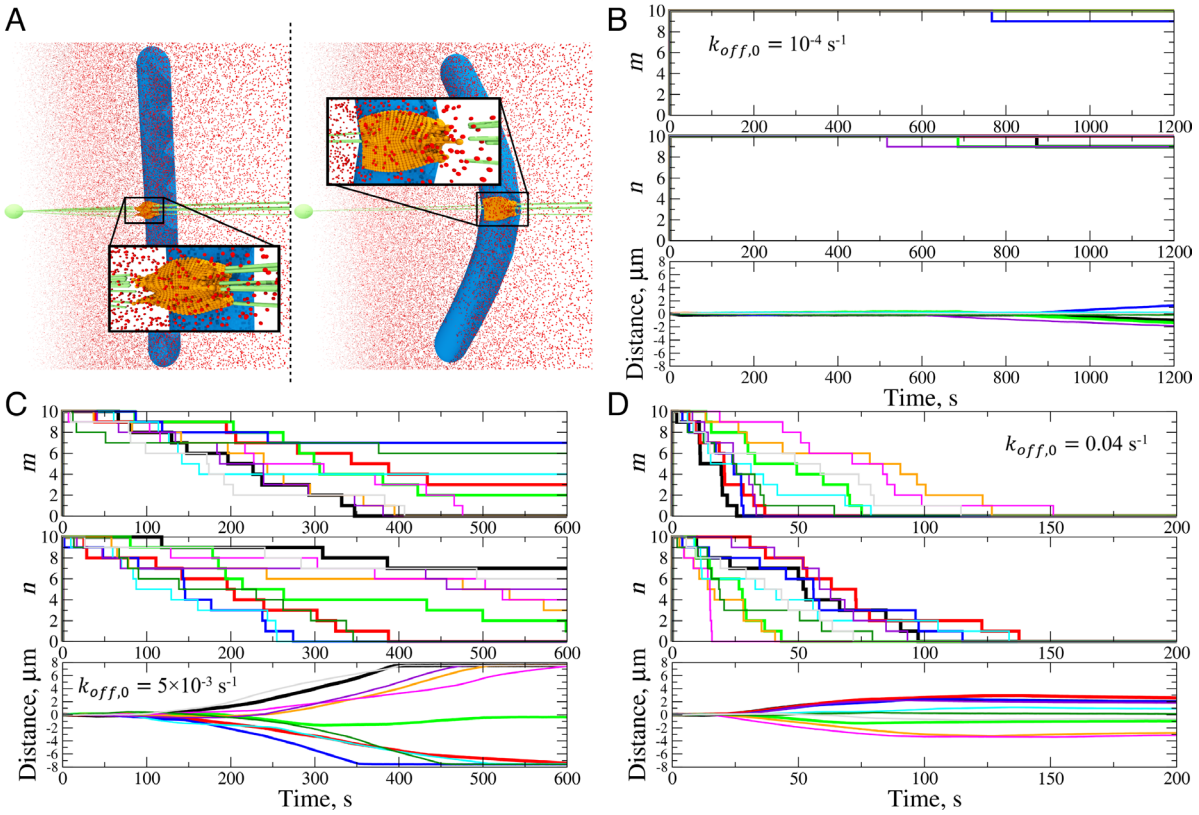

Fig. 5. Full 3D simulations of a single chromatid using CellDynaMo for a symmetric merotelic attachment: (*A*) Snapshots from CellDynaMo simulations illustrating the initial state ($m = n = 10$, *Left*) and an intermediate state ($m = 3$ and $n = 5$, *Right*). (*B–D*) Numbers of MTs from the left pole m, from the right pole n, and the distance from the chromatid to the equatorial plate as functions of time for equal initial numbers of MTs from both poles, i.e., MT ratio m: $n = 10$: 10, and for $k_{off,0} = 10^{-4}s^{-1}$ (*B*), $k_{off,0} = 5 \times 10^{-3}s^{-1}$ (*C*), and $k_{off,0} = 0.04\ s^{-1}$ (*D*). For each case (*B*, *C*, and *D*), results of 10 simulation runs are shown in different colors.

improves significantly. Indeed, in healthy cells, error correction occurs at steady rates throughout mitosis, and error correction before anaphase is very effective (9). For example, if the average MT numbers at sister KTs are $m = 15$ and $n = 10$, then waiting for 5 min resolves 70 to 80% of the lagging chromatids, and increasing further the waiting time to 10 min resolves almost 90% of the lagging chromatids. Moreover, if the MT numbers at sister KTs are $m = 15$ and $n = 5$, then waiting for 5 min resolves ~90% of the lagging chromatids (*SI Appendix*). Note that although we are not explicitly addressing preanaphase merotelic corrections, in principle, the model applies to them as well and sheds light on optimal MT detachment frequencies before anaphase.

Thus, potentially the safest strategy in anaphase is to decrease the KT–MT detachment frequency at the spindle equator, as posited in Ref. 16, if anaphase is long enough and if partial early error correction has been done. One of the hypothetical mechanisms for such partial early error correction is suggested in Ref. 19: One or several incorrect MTs stretch deformable KTs, and the merotelic part of KT extends toward the inner centromere, where Aurora B is enriched in early mitosis, thus enabling rapid detachment of the incorrect MTs only. One relevant observation is that merotelic chromatids usually go to "correct" poles (41), meaning the pole opposite to the one attracting the sister chromatid, which suggests the asymmetry of the MT numbers connected to the merotelic KT, such that the MT majority comes from the correct pole. One additional benefit of the pure tug-of-war strategy is not losing the lagging chromatids with a small initial total number of MTs.

Symmetric merotelic connections were often observed stuck at the spindle equator (11, 12, 16), also supporting indirectly the pure tug-of-war mechanism; however, statistics and quantification in these studies are limited, and additional experiments on measuring dynamic MT numbers from the opposite poles will be needed to discriminate between several potential error correction mechanisms. Without such measurements, viability of the pure tug-of-war mechanism remains an open question (16, 17).

If the cell only "cares" about asymmetric merotelic attachments, for which the spatial profile of the detachment rate is irrelevant, why then is Aurora B enriched at the spindle equator in anaphase? A possible answer, suggested in Ref. 17, is that the Aurora B–generated phosphorylation gradient at the spindle equator assists kinesin-5-mediated antiparallel MT sliding at the equator, which increases the opposing forces on the merotelic chromatids assisting the tug-of-war mechanically. This illustrates that the models we explored here are relatively simplistic, ignoring the complex structure of the spindle MT network (42) and molecular pathways of the error correction processes (20).

However, some of these complexities can be explored with simple 1D model estimates. Namely, first, we simulated additional mechanical resistance to the movement of the lagging chromatid from spindle elements at the equator and found that this factor has relatively little effect on the results (*SI Appendix*). Second, it was shown in vitro that the force–velocity relations could be different for the growing and shortening MTs (31). We varied these force–velocity relations accordingly and found again that qualitatively the results did not change (*SI Appendix*, Fig. S5 *A–C*). Last, but not least, in vitro data suggest that force dependencies of the KT–MT dissociation rates could be different for the growing and shortening MTs (31) (*SI Appendix*, Fig. S5 *D–F* and *Supporting text*). We explored these differences and found that, intuitively, if KT–MT bonds have the catch character for the shortening MT majority but the slip character for the growing MT minority, then error correction becomes more robust (*SI Appendix*, Fig. S5*D*). The

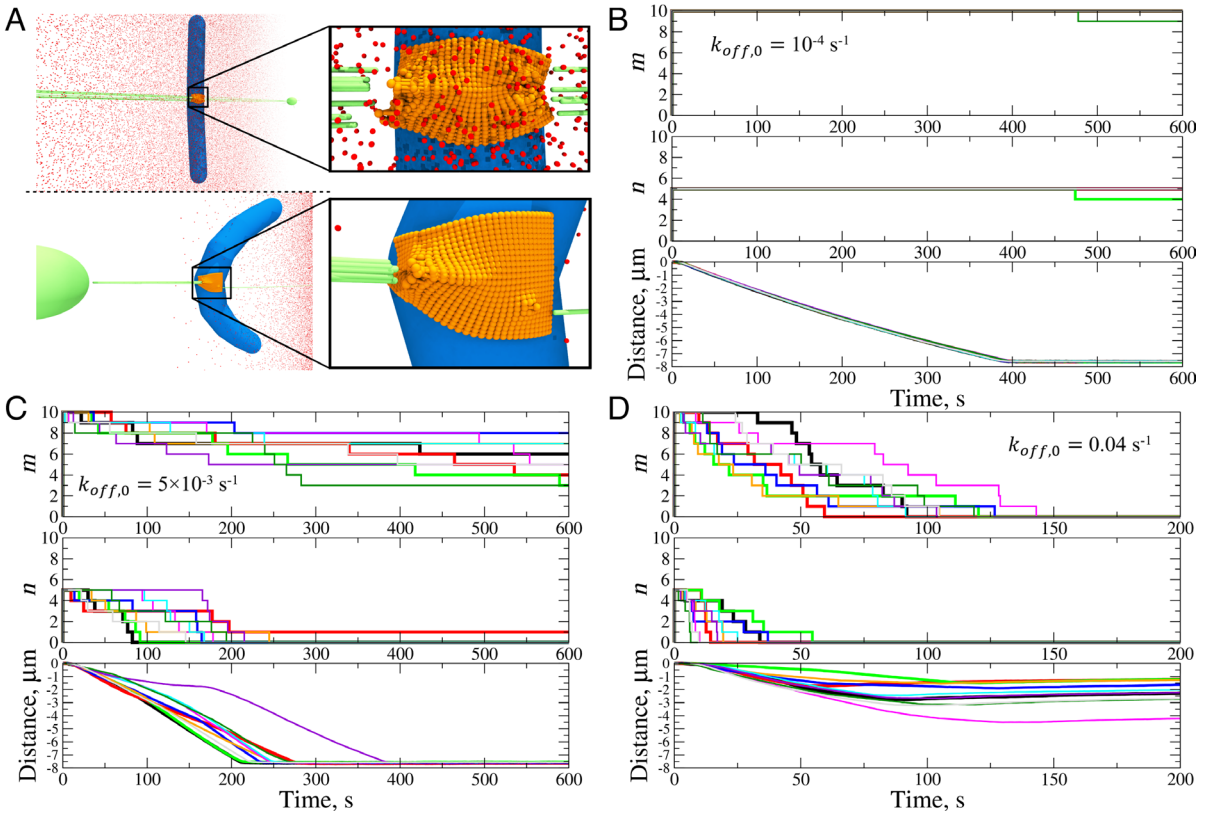

Fig. 6. Full 3D simulations of a single chromatid using CellDynaMo for an asymmetric merotelic attachment: (*A*) Snapshots from CellDynaMo simulations illustrating the initial state ($m = 10$ and $n = 5$, *Top*) and an intermediate state ($m = 6$ and $n = 1$, *Bottom*). (*B–D*) Numbers of MTs from the *Left* pole m, from the right pole n, and the distance from the chromatid to the equatorial plate as functions of time for unequal initial numbers of MTs from both poles, i.e., MT ratio m: $n = 10$: 5, and for $k_{off,0} = 10^{-4} s^{-1}$ (*B*), $k_{off,0} = 5 \times 10^{-3} s^{-1}$ (*C*), and $k_{off,0} = 0.004\ s^{-1}$ (*D*). For each case (*B*, *C*, and *D*), results of 10 simulation runs are shown in different colors.

opposite situation ruins the error correction process completely (*SI Appendix*, Fig. S5*E*). Finally, if all KT–MT bonds are catch-slip-like, the error correction improves because the shortening MT majority operates at smaller force per MT in the catch regime in this case, while the growing MT minority—in the slip regime (*SI Appendix*, Fig. S5*F*).

Finally, if there are many symmetric and slightly asymmetric merotelic attachments at the onset of anaphase, then increasing and fine-tuning the KT–MT detachment rate near the equator, as is suggested in Ref. 16, could become the optimal strategy. Our simulations suggest that the optimal KT–MT detachment rate is ~ 0.005 s^{-1} (Fig. 5). This prediction is remarkably close to the estimate made in Ref. 17 that about 50% of MTs turn over within ~5 min in anaphase, which indicates that the observed KT–MT detachment rate is ~ 0.003 s^{-1}. In support of this result, it was observed that even slight changes in KT–MT dynamics might lead to chromosomal instability (15). Furthermore, both depletion and inhibition of Aurora B in cancer cells were demonstrated to produce lagging chromosomes (43, 44), which is consistent with the predicted need to fine-tune the Aurora B gradient for the optimal regime of moving laggards away from the spindle equator.

Data, Materials, and Software Availability. All study data are included in the article and/or *SI Appendix*.

ACKNOWLEDGMENTS. We thank H. Maiato and A. Khodjakov for useful discussions. A.M. was supported by NSF grant DMS 1953430. V.B. was supported in part by NIH Research Project Grant Program (R01) grant HL148227. Portions of the paper were developed from the thesis of E.K.

Author affiliations: [a]Department of Chemistry, University of Massachusetts, Lowell, MA 01854; and [b]Courant Institute for Mathematical Sciences and Department of Biology, New York University, New York, NY 10012

1. S. Dumont, T. J. Mitchison, Force and length in the mitotic spindle. *Curr. Biol.* **19**, R749–R761 (2009).
2. J. M. Scholey, G. Civelekoglu-Scholey, I. Brust-Mascher, Anaphase b. *Biology (Basel)* **5**, 51 (2016).
3. C. L. Asbury, Anaphase A: Disassembling microtubules move chromosomes toward spindle poles. *Biology (Basel)* **6**, 15 (2017).
4. K. Vukušić, R. Buđa, I. M. Tolić, Force-generating mechanisms of anaphase in human cells. *J. Cell Sci.* **132**, jcs231985 (2019).
5. R. Heald, A. Khodjakov, Thirty years of search and capture: The complex simplicity of mitotic spindle assembly. *J. Cell Biol.* **211**, 1103–1111 (2015).
6. M. A. Lampson, E. L. Grishchuk, Mechanisms to avoid and correct erroneous kinetochore-microtubule attachments. *Biology (Basel)* **6**, 1 (2017).
7. R. Paul *et al.*, Computer simulations predict that chromosome movements and rotations accelerate mitotic spindle assembly without compromising accuracy. *Proc. Natl. Acad. Sci. U.S.A.* **106**, 15708–15713 (2009).
8. W. T. Silkworth, I. K. Nardi, R. Paul, A. Mogilner, D. Cimini, Timing of centrosome separation is important for accurate chromosome segregation. *Mol. Biol. Cell* **23**, 401–411 (2012).
9. G. Ha, P. Dieterle, H. Shen, A. Amir, D. J. Needleman, Measuring and modeling the dynamics of mitotic error correction. *Proc. Natl. Acad. Sci. U.S.A.* **121**, e2323009121 (2024).
10. A. D. Silk *et al.*, Chromosome missegregation rate predicts whether aneuploidy will promote or suppress tumors. *Proc. Natl. Acad. Sci. U.S.A.* **110**, E4134–E4141 (2013).
11. D. Cimini, B. Moree, J. C. Canman, E. D. Salmon, Merotelic kinetochore orientation occurs frequently during early mitosis in mammalian tissue cells and error correction is achieved by two different mechanisms. *J. Cell Sci.* **116**, 4213–4225 (2003).
12. D. Cimini, L. A. Cameron, E. D. Salmon, Anaphase spindle mechanics prevent mis-segregationof merotelically oriented chromosomes. *Curr. Biol.* **14**, 2149–2155 (2004).
13. A. Kouznetsova, T. S. Kitajima, H. Brismar, C. Höög, Post-metaphase correction of aberrant kinetochore-microtubule attachments in mammalian eggs. *EMBO Rep.* **20**, e47905 (2019).
14. S. L. Thompson, D. A. Compton, Chromosome missegregation in human cells arises through specific types of kinetochore–microtubule attachment errors. *Proc. Natl. Acad. Sci.* **108**, 17974–17978 (2011).

15. S. F. Bakhoum, S. L. Thompson, A. L. Manning, D. A. Compton, Genome stability is ensured by temporal control of kinetochore-microtubule dynamics. *Nat. Cell Biol.* **11**, 27–35 (2009).
16. B. Orr *et al.*, An anaphase surveillance mechanism prevents micronuclei formation from frequent chromosome segregation errors. *Cell Rep.* **37**, 109783 (2021).
17. O. Sen, J. U. Harrison, N. J. Burroughs, A. D. McAinsh, Kinetochore life histories reveal an Aurora-B-dependent error correction mechanism in anaphase. *Dev. Cell* **56**, 3082–3099 (2021).
18. E. D. Salmon, D. Cimini, L. A. Cameron, J. G. DeLuca, Merotelic kinetochores in mammalian tissue cells. *Philos. Trans. R. Soc. B Biol. Sci.* **360**, 553–568 (2005).
19. D. Cimini, X. Wan, C. B. Hirel, E. D. Salmon, Aurora kinase promotes turnover of kinetochore microtubules to reduce chromosome segregation errors. *Curr. Biol.* **16**, 1711–1718 (2006).
20. H. Maiato, S. Silva, Double-checking chromosome segregation. *J. Cell Biol.* **222**, e202301106 (2023).
21. G. Gay, T. Courtheoux, C. Reyes, S. Tournier, Y. Gachet, A stochastic model of kinetochore-microtubule attachment accurately describes fission yeast chromosome segregation. *J. Cell Biol.* **196**, 757–774 (2012).
22. E. S. Tubman, S. Biggins, D. J. Odde, Stochastic modeling yields a mechanistic framework for spindle attachment error correction in budding yeast mitosis. *Cell Syst.* **4**, 645–650 (2017).
23. G. Civelekoglu-Scholey *et al.*, Dynamic bonds and polar ejection force distribution explain kinetochore oscillations in PtK1 cells. *J. Cell Biol.* **201**, 577–593 (2013).
24. M. A. C. Medina, K. Iemura, A. Kimura, K. Tanaka, A mathematical model of kinetochore-microtubule attachment regulated by Aurora A activity gradient describes chromosome oscillation and correction of erroneous attachments. *Biomed. Res.* **42**, 203–219 (2021).
25. D. Cimini *et al.*, Merotelic kinetochore orientation is a major mechanism of aneuploidy in mitotic mammalian tissue cells. *J. Cell Biol.* **153**, 517–528 (2001).
26. Y. Zhai, P. J. Kronebusch, G. G. Borisy, Kinetochore microtubule dynamics and the metaphase–anaphase transition. *J. Cell Biol.* **131**, 721–734 (1995).
27. G. J. Gorbsky, P. J. Sammak, G. G. Borisy, Chromosomes move poleward in anaphase along stationary microtubules that coordinately disassemble from their kinetochore ends. *J. Cell Biol.* **104**, 9–18 (1987).
28. A. F. Long, P. Suresh, S. Dumont, Individual kinetochore-fibers locally dissipate force to maintain robust mammalian spindle structure. *J. Cell Biol.* **219**, e201911090 (2020).
29. G. I. Bell, Models for the specific adhesion of cells to cells: A theoretical framework for adhesion mediated by reversible bonds between cell surface molecules. *Science* **200**, 618–627 (1978).
30. A. Kunwar, A. Mogilner, Robust transport by multiple motors with nonlinear force–velocity relations and stochastic load sharing. *Phys. Biol.* **7**, 16012 (2010).
31. B. Akiyoshi *et al.*, Tension directly stabilizes reconstituted kinetochore-microtubule attachments. *Nature* **468**, 576–579 (2010).
32. G. Cojoc *et al.*, Laser microsurgery reveals conserved viscoelastic behavior of the kinetochore. *J. Cell Biol.* **212**, 767–776 (2016).
33. S. Dumont, E. D. Salmon, T. J. Mitchison, Deformations within moving kinetochores reveal different sites of active and passive force generation. *Science* **337**, 355–358 (2012).
34. E. Kliuchnikov, A. Zhmurov, K. A. Marx, A. Mogilner, V. Barsegov, Cell DynaMo – stochastic reaction–diffusion-dynamics model: Application to search-and-capture process of mitotic spindle assembly. *PLoS Comput. Biol.* **18**, e1010165 (2022).
35. E. Kliuchnikov, K. A. Marx, A. Mogilner, V. Barsegov, Interrelated effects of chromosome size, mechanics, number, location-orientation and polar ejection force on the spindle accuracy: A 3D computational study. *Mol. Biol. Cell* **34**, ar57 (2023).
36. P. Meraldi, V. M. Draviam, P. K. Sorger, Timing and checkpoints in the regulation of mitotic progression. *Dev. Cell* **7**, 45–60 (2004).
37. J. Allard, M. Doumic, A. Mogilner, D. Oelz, Bidirectional sliding of two parallel microtubules generated by multiple identical motors. *J. Math. Biol.* **79**, 571–594 (2019).
38. T. Courtheoux, G. Gay, Y. Gachet, S. Tournier, Ase1/Prc1-dependent spindle elongation corrects merotely during anaphase in fission yeast. *J. Cell Biol.* **187**, 399–412 (2009).
39. D. Dudka *et al.*, Complete microtubule–kinetochore occupancy favours the segregation of merotelic attachments. *Nat. Commun.* **9**, 2042 (2018).
40. B. F. McEwen *et al.*, CENP-E is essential for reliable bioriented spindle attachment, but chromosome alignment can be achieved via redundant mechanisms in mammalian cells. *Mol. Biol. Cell* **12**, 2776–2789 (2001).
41. S. L. Thompson, D. A. Compton, Examining the link between chromosomal instability and aneuploidy in human cells. *J. Cell Biol.* **180**, 665–672 (2008).
42. C.-H. Yu *et al.*, Central-spindle microtubules are strongly coupled to chromosomes during both anaphase A and anaphase B. *Mol. Biol. Cell* **30**, 2503–2514 (2019).
43. K. Pfister *et al.*, Identification of drivers of aneuploidy in breast tumors. *Cell Rep.* **23**, 2758–2769 (2018).
44. E. Britigan *et al.*, Increased Aurora B expression reduces substrate phosphorylation and induces chromosomal instability. *Front. Cell Dev. Biol.* **10**, 1018161 (2022).